HUMAN GENE THERAPY 18:401–412 (May 2007)

DOI: 10.1089/hum.2006.161

Chemical Dimerization of Fibroblast Growth Factor Receptor-1 Induces Myoblast Proliferation, Increases Intracardiac Graft Size, and Reduces Ventricular Dilation in Infarcted Hearts

KELLY R. STEVENS,[1,2,*] MARSHA W. ROLLE,[3,*] ELINA MINAMI,[2,4] SHUICHI UENO,[2] MARILYN B. NOURSE,[1,2] JITKA I. VIRAG,[5] HANS REINECKE,[2] and CHARLES E. MURRY[1,2]

ABSTRACT

The ability to control proliferation of grafted cells in the heart and consequent graft size could dramatically improve the efficacy of cell therapies for cardiac repair. To achieve targeted graft cell proliferation, we created a chimeric receptor (F36Vfgfr-1) composed of a modified FK506-binding protein (F36V) fused with the cytoplasmic domain of the fibroblast growth factor receptor-1 (FGFR-1). We retrovirally transduced mouse C2C12 and MM14 skeletal myoblasts with this construct and treated them with AP20187, a dimeric F36V ligand ("dimerizer"), *in vitro* and *in vivo* to induce receptor dimerization. Dimerizer treatment *in vitro* activated the mitogen-activated protein kinase pathway and induced proliferation in myoblasts expressing F36Vfgfr-1 comparable with the effects of basic FGF. Wild-type myoblasts did not respond to dimerizer. Subcutaneous grafts composed of myoblasts expressing F36Vfgfr-1 showed a dose-dependent increase in DNA synthesis with dimerizer treatment. When myoblasts expressing F36Vfgfr-1 were injected into infarcted hearts of nude mice, dimerizer treatment resulted in a dose-dependent increase in graft size, from 20 ± 3 to 42.9 ± 4.3% of the left ventricle. Blinded echocardiographic analysis demonstrated that larger graft size was associated with a dose-dependent reduction in ventricular dilation after myocardial infarction, although animals with the largest grafts showed an increased incidence of ventricular tachycardia. Thus, selective proliferation of genetically modified graft cells can be induced with a systemically administered synthetic molecule *in vitro* or *in vivo*. Control of intramyocardial graft size by this approach may allow optimization of cell-based therapy to obtain desired cardiac function postinfarction.

INTRODUCTION

CELL GRAFTS FOR CARDIAC REPAIR must replace a substantial portion of the infarcted myocardium if they are to be maximally therapeutic. A positive correlation between the number of injected cells and the magnitude of cardiac functional improvement has been shown, indicating that larger grafts have a greater impact on left ventricular function (Pouzet *et al*., 2001; Tambara *et al*., 2003). In most applications, intracardiac cell grafts are small (Li *et al*., 1996) and show considerable graft-to-graft variability. Graft size is determined by the number of cells injected, the fraction of cells that is retained, the extent of cell death after grafting, and the proliferation of viable cells. Strategies to increase initial cell number, increase cell retention, or prevent cell death show promise (Suzuki *et al*., 2000; Zhang *et al*., 2001; Mangi *et al*., 2003; Yau *et al*., 2004), but these strategies can, at best, increase graft size linearly. Augmentation of graft cell proliferation promises exponential graft expansion. Furthermore, controlled graft cell proliferation postimplantation could allow adjustment of graft size based on initial engraftment success. It also would allow concurrent vascular and extracellular matrix remodeling, which could support

[1]Department of Bioengineering, University of Washington, Seattle, WA 98195.
[2]Center for Cardiovascular Biology, Institute for Stem Cell and Regenerative Medicine, and Department of Pathology, University of Washington, Seattle, WA 98109.
[3]Benaroya Research Institute, Seattle, WA 98101.
[4]Division of Cardiology, Department of Medicine, University of Washington, Seattle, WA 98195.
[5]Brody School of Medicine, East Carolina University, Greenville, NC 27858.
*K.R.S. and M.W.R. contributed equally to this work.

the success of the graft. For these reasons, our group is developing systems to control graft cell proliferation (Whitney *et al*., 2001).

Skeletal muscle satellite cells, or myoblasts, represent an excellent candidate cell type for developing a system to enhance the proliferation of intracardiac graft cells. Myoblasts have been extensively studied in cardiac repair, are the subject of ongoing clinical trials, and have basal proliferative ability (Koh *et al*., 1993; Murry *et al*., 1996, 2005). Myoblast proliferation is stimulated by basic fibroblast growth factor (bFGF, FGF-2), which also prevents their differentiation into myotubes (Templeton and Hauschka, 1992; Milasincic *et al*., 1996). Direct administration of bFGF to intramyocardial grafts, however, might also stimulate host tissue fibroblasts and cause undesirable fibrosis (Boilly *et al*., 2000; Whitney *et al*., 2001). We therefore developed a system to target selective expansion of genetically modified myoblasts without stimulating endogenous host cells (Whitney *et al*., 2001). A chimeric, drug-responsive growth factor receptor (F36Vfgfr-1) (Whitney *et al*., 2001), which contains a modified FK506-binding protein (F36V) (Clackson *et al*., 1998) and the cytoplasmic domain of the fibroblast growth factor receptor-1 (FGFR-1), was created. We showed that chemical dimerization of FGFR-1 mimicked FGF signaling pathways in skeletal myoblasts, including activation of the mitogen-activated protein (MAP) kinase pathway and stimulation of proliferation, and that this effect was reversible on ligand withdrawal (Whitney *et al*., 2001).

In the present study, we apply the F36Vfgfr-1 strategy to the *in vivo* control of intracardiac graft size in infarcted mouse hearts. We first test whether chemical dimerization of F36Vfgfr-1 in C2C12 skeletal myoblasts stimulates cell proliferation via the MAP kinase signaling pathway *in vitro*. We then show that systemic delivery of dimerizer to mice with subcutaneous or intracardiac grafts of F36Vfgfr-1 myoblasts results in targeted stimulation of graft cell proliferation *in vivo*, increased graft size, and a dose-dependent reduction in ventricular dilation after myocardial infarction. Selective graft cell expansion using this system may allow fine-tuning of intramyocardial graft size posttransplantation to attenuate left ventricular dilation and improve cardiac function.

MATERIALS AND METHODS

F36Vfgfr-1 plasmid construction and retrovirus production

Molecular cloning of the chimeric receptor, F36Vfgfr-1, was described in detail previously (Whitney *et al*., 2001). Briefly, F36Vfgfr-1 (Fig. 1A) is composed of a c-Src myristoylation domain, the modified FK506-binding protein (FKBP) domain (F36V), the cytoplasmic domain of rat FGFR-1, and a hemagglutinin epitope tag (HA.11). This construct was ligated into a bicistronic expression vector containing an internal ribosome entry sequence (IRES) preceded by the enhanced green fluorescent protein (EGFP) reporter gene. Expression of the fusion gene and EGFP was driven by the murine stem cell virus long terminal repeat (MSCV LTR). PA317 amphotropic retroviral packaging cells stably expressing the F36Vfgfr-1 construct were generated and purified with a BD FACSAria cell-sorting system (BD Biosciences, San Jose, CA) based on EGFP expression. Purified PA317 cells were expanded in culture and supernatants were collected for myoblast transduction.

Culture, transduction, and purification of F36Vfgfr-1 myoblasts

Murine MM14 skeletal myoblasts stably expressing the F36Vfgfr-1 chimeric receptor were generated by retroviral transduction, purified by flow cytometry based on EGFP expression, and expanded in growth medium (Ham's F10 medium [Invitrogen, Carlsbad, CA], 15% horse serum [MP Biomedicals, Irvine, CA], bFGF [6 ng/ml; kindly donated by Scios, Moun-

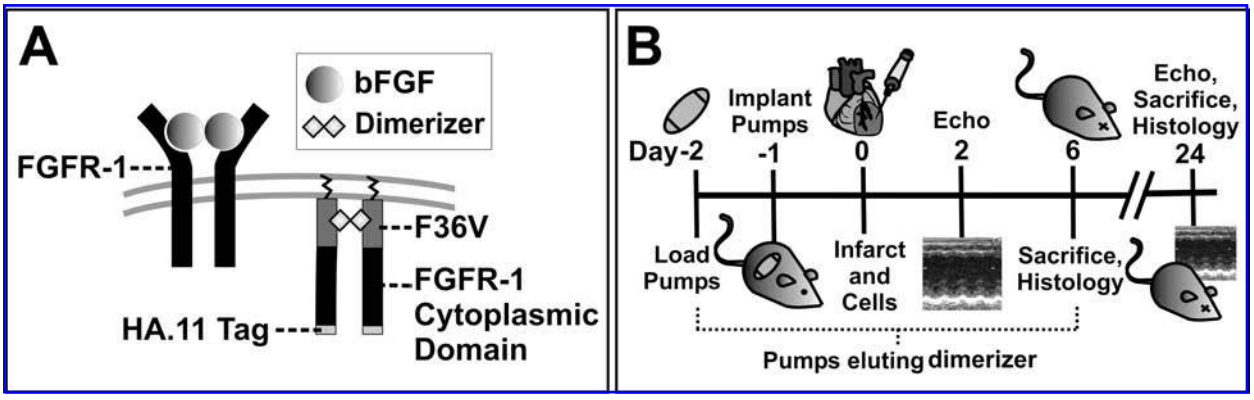

FIG. 1. Schematics of signaling control system and experimental design. (**A**) The chimeric F36Vfgfr-1 receptor is composed of an F36V drug-binding domain fused to the cytoplasmic domain of the FGFR-1 receptor. Dimerizer binding to the F36V domain results in dimerization and receptor *trans*-phosphorylation (*right*) similar to bFGF-induced activation of FGFR-1 (*left*). Also shown are the HA.11 epitope tag and the c-Src myristoylation domain of the chimeric receptor. (**B**) Intracardiac grafting experiment design. Osmotic pumps delivering dimerizer or vehicle only were implanted subcutaneously into the backs of nude mice. On day 0, the coronary artery was ligated and C2C12 myoblasts transfected with the chimeric F36Vfgfr-1 receptor were injected into the infarcted zone. Echocardiography was performed on day 2 and day 24. Animals were killed on day 6 or 24 for histology and morphometric analysis.

tain View, CA], penicillin G [100 units/ml], streptomycin [100 μg/ml], and amphotericin B [0.25 μg/ml] [Invitrogen]) on gelatin-coated plates (Whitney *et al*., 2001). Murine C2C12 skeletal myoblasts (a gift from S. Hauschka, Department of Biochemistry, University of Washington, Seattle, WA) were cultured in C2C12 growth medium (Dulbecco's modified Eagle's medium [DMEM; Invitrogen], 20% fetal bovine serum [FBS; HyClone, Logan, UT], 2 m*M* L-glutamine [Invitrogen], penicillin G [100 units/ml], streptomycin [100 μg/ml], and amphotericin B [0.25 μg/ml] [Invitrogen GIBCO, Grand Island, NY]) on 0.67% gelatin-coated tissue culture dishes. C2C12 cells were plated into gelatin-coated 6-well plates, transduced by incubation with PA317 F36Vfgfr-1 retroviral supernatant supplemented with 20% FBS and Polybrene (8 μg/ml; Sigma, St. Louis, MO), and centrifuged for 30 min at 2500 rpm (1180 × *g*). Retroviral supernatant was removed and replaced with fresh growth medium. Stably transduced C2C12 F36Vfgfr-1 cells were isolated by flow cytometry based on EGFP expression and expanded in C2C12 growth medium.

Proliferation assays

C2C12 F36Vfgfr-1 or C2C12 wild-type cells were cultured in C2C12 growth medium and then replated at a density of 10,000 cells per well into gelatin-coated 24-well plates. After replating, cells were incubated in basal medium containing DMEM, 0.5% FBS, 2 m*M* L-glutamine, penicillin G (100 units/ml), streptomycin (100 μg/ml), and amphotericin B (0.25 μg/ml) and various treatments. To test the effect of dimerizer (AP20187; donated by ARIAD Pharmaceuticals, Cambridge, MA) on C2C12 wild-type and C2C12 F36Vfgfr-1 cells, cells were treated with bFGF (6 ng/ml), received no treatment, or were treated with 100 n*M* dimerizer for 48 hr. The medium was then removed and replaced with 400 μl of DMEM and 40 μl of 3-(4,5-dimethythiazol-2-yl)-2,5-diphenyltetrazolium bromide (MTT, 5 mg/ml; Sigma) per well. After 4 hr of incubation, the cells were lysed with 550 μl of lysis buffer (10% sodium dodecyl sulfate [SDS], 0.1 *M* HCl). Relative MTT conversion levels in the samples were measured by spectrophotometry ($\lambda = 570$ nm). We noticed that basal proliferation rates differed between the parental C2C12 cells and the F36Vfgfr-1-expressing cells (basal proliferation was ~25% lower in F36Vfgfr-1-expressing cells). To correct for this, absorbance levels were normalized to the mean absorbance of FGF-treated control wells for each respective cell type in order to clearly test the effect of dimerizer (relative to bFGF) on each cell type.

In a second study, C2C12 F36Vfgfr-1 cells were treated in basal medium containing 0, 1, 10, or 100 n*M* dimerizer with or without 10 μ*M* U0126 (Promega, Madison, WI), an MEK (MAPK/ERK kinase) inhibitor, to study the dose dependence of dimerizer and to test whether proliferation stimulated by dimerizer was activated via the MAP kinase signaling pathway. After 48 hr, the medium in each well was removed and replaced with 500 μl of basal medium containing 10% (v/v) Alamar Blue (Invitrogen Biosource, Camarillo, CA). After 4 hr of incubation, 100 μl of solution from each well was placed into a 96-well plate and a microplate reader (Safire^2; Tecan Group, Maennedorf, Switzerland) was used to measure fluorescence intensity (excitation $\lambda = 530$ nm, emission $\lambda = 590$ nm). Relative fluorescence was normalized to the mean fluorescence of 100 n*M* AP20187-treated wells. Statistical significance ($p < 0.05$) for all proliferation studies was determined by two-tailed Student *t* test, assuming unequal variance.

Western blotting

C2C12 F36Vfgfr-1 and C2C12 wild-type cells were cultured in growth medium in 150-mm gelatin-coated plates. Cells were serum starved (DMEM, 0.2% bovine serum albumin [BSA; MP Biomedicals], 2 m*M* L-glutamine [Invitrogen], penicillin G [100 units/ml], streptomycin [100 μg/ml], and amphotericin B [0.25 μg/ml] [Invitrogen GIBCO]) overnight and then incubated for 15 min with bFGF (6 ng/ml), 100 n*M* dimerizer, or left untreated. In a separate experiment, cells were incubated for 15 min with 0, 1, 10, or 100 n*M* dimerizer with or without a 15 μ*M* concentration of the MEK inhibitor U0126. Plates were washed twice with ice-cold phosphate-buffered saline (PBS; Invitrogen) before lysis in sample buffer (50 m*M* Tris-HCl, 1% SDS, 10% glycerol) containing phosphatase inhibitors (1 m*M* sodium fluoride, 1 m*M* sodium pyrophosphate, and 1 m*M* sodium orthovanadate) and complete EDTA-free protease inhibitor cocktail (1×; Roche Applied Science, Indianapolis, IN). Lysed cells were homogenized by passage through a 22-gauge needle 10 times to shear genomic DNA. Cell lysate protein concentration was assayed with a Micro BCA kit (Pierce Biotechnology, Rockford, IL) for assurance of equal loading. Protein lysates (25 μg/lane) were loaded into a 10% polyacrylamide gel, separated by SDS–polyacrylamide gel electrophoresis, and transferred to an Immobilon-FL polyvinylidene difluoride (PVDF) transfer membrane (Millipore, Bedford, MA). The membrane was blocked with blocking buffer (20 m*M* Tris-HCl, 500 m*M* NaCl, 0.05% Tween 20, and 5% Carnation nonfat dry milk) for 1 hr at room temperature and incubated with a polyclonal antibody against phosphorylated extracellular signal-regulated kinase (ERK)-1/2 (1:1000; Cell Signaling Technology, Danvers, MA) overnight at 4°C. Identical blots were prepared and incubated with an antibody against total ERK-1/2 (pan-ERK, diluted 1:1000; Chemicon International/Millipore, Temecula, CA) overnight at 4°C. The membranes were rinsed in TBS-T (20 m*M* Tris-HCl [pH 7.8], 300 m*M* NaCl, 0.1% Tween 20) and incubated with secondary antibody (horseradish peroxidase-conjugated goat anti-rabbit, diluted 1:7500 for phosphorylated ERK-1/2 and 1:50,000 for pan-ERK-1/2; Jackson ImmunoResearch Laboratories, West Grove, PA) for 1 hr at room temperature before development with a chemiluminescent reagent (SuperSignal West Dura; Pierce Biotechnology) and exposure to Hyperfilm ECL film (GE Healthcare Life Sciences, Piscataway, NJ).

In vivo *subcutaneous ectopic graft model*

All animal procedures described were reviewed and approved by the University of Washington (Seattle, WA) Institutional Animal Care and Use Committee and performed in accordance with federal guidelines for the care and use of laboratory animals. Implantable osmotic pumps (model 1007 D; Alzet, Cupertino, CA) were filled with dimerizer dissolved in PEG 400 (Sigma) at concentrations yielding elution rates of 0, 9.6, or 24 mg/kg/day. Pumps were incubated at 37°C in sterile PBS for 6 hr to initiate pump elution (pumps elute 0.5 μl/hr over the course of 7 days). Pumps then were implanted subcutaneously into the backs of male nude mice (Charles River Lab-

oratories, Wilmington, MA) under ether anesthesia ($n = 2$ mice per dimerizer dose). The next day, MM14 F36Vfgfr-1 cells were injected subcutaneously to form ectopic muscle grafts ($n = 3$ or 4 grafts per mouse; 5×10^6 cells per graft). Six days after subcutaneous cell transplantation, mice were injected intraperitoneally with 0.2 ml of bromodeoxyuridine (BrdU, 10 mg/ml; Roche Applied Science) 1 hr before sacrifice. Ectopic grafts were harvested, fixed in methyl Carnoy's solution (60% methanol, 30% chloroform, 10% glacial acetic acid), embedded in paraffin, and sectioned for histological evaluation. Graft sections were double-stained for desmin expression and BrdU incorporation. Sections were quenched for 30 min in methanol with 0.3% hydrogen peroxide (MeOH–H_2O_2), blocked with 1.5% normal horse serum, and incubated for 1 hr in undiluted horseradish peroxidase (HRP)-conjugated mouse anti-desmin primary antibody (Dako, Carpinteria, CA). Desmin staining was visualized with diaminobenzidine substrate (DAB; Vector Laboratories, Burlingame, CA) resulting in brown cytoplasmic staining. Sections were quenched a second time in MeOH–H_2O_2 for 30 min and rinsed in water. BrdU antigen retrieval was performed by incubation in 1.5 *N* HCl for 15 min at 37°C followed by two washes in 0.1 *M* borax buffer (pH 8.5) and two washes in PBS for neutralization. Sections were then incubated with HRP-conjugated anti-BrdU antibody (1:25, Roche Applied Science) overnight at 4°C. Nuclear incorporation of BrdU was visualized with Vector VIP substrate (Vector Laboratories) to give a dark blue nuclear stain. Sections were counterstained with methyl green and coverslipped with Permount (Fisher Scientific, Hampton, NH). For each graft, 1000 desmin-positive nuclei accumulated from 8 separate fields of view were counted. The number of BrdU-labeled nuclei in these desmin-positive cells was recorded to determine the percentage of graft cells in S phase. A two-tailed unequal variance Student *t* test was performed to determine whether the difference in the percentage of BrdU-positive cells in untreated compared with dimerizer-treated grafts was significant.

Coronary artery ligation and intracardiac grafting model

The timeline for these experiments is shown in Fig. 1B. Implantable osmotic pumps eluting dimerizer dissolved in PEG 400 at 0, 9.6, or 24 mg/kg/day were incubated in sterile saline at 37°C overnight to initiate pump elution. The next day, these pumps were implanted subcutaneously into the backs of male nude mice under isoflurane anesthesia. On the day after pump implantation, myocardial infarction was induced by permanent coronary artery ligation, and cell injection was performed as detailed previously by our group (Reinecke *et al*., 2002; Virag and Murry, 2003). Briefly, mice were anesthetized and mechanically ventilated. The chest was opened and the left anterior descending coronary artery was ligated with an 8-0 suture. C2C12 F36Vfgfr-1 cells were then injected directly into the infarcted left ventricular free wall, using a 30-gauge needle. Two injections of 50,000 cells per 3.5 μl of grafting medium (serum- and antibiotic-free DMEM) were performed to maximize the dispersion of cells throughout the infarcted region. Sham-engrafted animals (administered dimerizer at 24 mg/kg/day) received two injections of 3.5 μl of grafting medium without cells. The chest was then closed aseptically, and animal recovery from surgery was monitored in a heated chamber.

Histologic and morphometric analysis of intracardiac graft size and myocardial fibrosis

Hearts were fixed and sectioned for histological analysis 6 days after cell injection, a time point immediately following the termination of dimerizer delivery (Fig. 1B). Hearts from animals killed 24 days after cell injection were also fixed and sectioned (Vibratome, St. Louis, MO) into slices 1 mm thick for histological analysis of the longer term effects of dimerizer. All sections were processed and paraffin embedded. Grafts were identified by immunohistochemistry, using a mouse monoclonal antibody against embryonic skeletal myosin (hybridoma supernatant, diluted 1:100) (F1.652, Developmental Studies Hybridoma Bank, University of Iowa, Iowa City, IA). Sections were blocked with 1.5% normal goat serum in PBS and incubated for 1 hr at room temperature with the biotinylated primary antibody (ARK [Animal Research Kit]; Dako). Sections were then incubated for 30 min at room temperature with HRP-conjugated streptavidin (Dako), developed with 3,3′-diaminobenzidine (DAB; Sigma), and counterstained with hematoxylin (Sigma). Photographs of heart sections were taken with a light microscope (Olympus BX41; Olympus America, Melville, NY) and a SPOT RT digital camera (Diagnostic Instruments, Sterling Heights, MI). The embryonic myosin-positive graft in every section of each heart was outlined in Photoshop (Adobe, San Jose, CA). Pixel counts were obtained for the outlined areas. The left ventricle was then similarly outlined in every section, and total pixel counts were determined. All pixel counts were converted to graft area and left ventricular area measurements, using a micrometer (Olympus America). Graft area was expressed as a percentage of left ventricular area. Heart sections were also stained with sirius red and fast green for identifying collagen fibers (red) and other tissue elements (green). Sections were rehydrated in a series of ethanol washes, stained in a solution of 0.1% sirius red (available for Sigma as Direct Red 80) and 0.1% fast green (Sigma) in 1.3% picric acid (Sigma), and dehydrated in a series of ethanol washes. The number of red pixels in every section of each graft was determined with Photoshop for quantification of total graft collagen. Total pixel counts from all graft sections were converted to area (mm^2) measurements, using a micrometer. Total graft collagen was then expressed as a percentage of graft area for a quantitative measurement of graft collagen density. Statistical significance ($p < 0.05$) was determined by two-tailed unequal variance Student *t* test.

Echocardiography

The effects of intracardiac cell injection and dimerizer treatment on left ventricular remodeling 2 and 24 days after coronary artery ligation were assessed by echocardiography. Mice were sedated with 1% isoflurane in 99% O_2 at a flow of 2 liters/min via a small nose cone and placed in a supine position on a 37°C heating pad. Electrocardiography (ECG) leads were placed on the paws of the animal to obtain simultaneous ECG tracings during imaging. Echocardiographic images were then obtained with a Vivid 7 Dimension system (GE Healthcare) using a 13-MHz linear array transducer. Parasternal long axis images were obtained first, followed by short-axis views at the midpapillary muscle level to acquire M-mode measurements of the left ventricular end-diastolic dimension (LVEDD) and left ventricular end-systolic dimension (LVESD). Data were aver-

aged from three to five cardiac cycles. All measurements were made in accordance with guidelines approved by the American Society of Echocardiography (Raleigh, NC) and were determined by a single echocardiographer, who was blinded to the treatment arms of the study. Statistical significance ($p < 0.05$) was determined by two-tailed Student *t* test, assuming unequal variance for comparing different groups at 24 days, and by two-tailed paired *t* test for comparing within groups between days 2 and 24. Animals in each group were also binned into "arrhythmia" or "no arrhythmia" binary categories based on ECG tracings at the time of echocardiography. Statistical significance ($p < 0.05$) between proportions of animals exhibiting arrhythmias in each treatment group was determined by Fisher exact test.

RESULTS

C2C12 F36Vfgfr-1 cells proliferate in response to dimerizer treatment in vitro

C2C12 wild-type and C2C12 F36Vfgfr-1 cells were cultured for 48 hr in the presence of bFGF (6 ng/ml), no treatment, or dimerizer to test the effect of dimerizer on each cell type. Relative cell numbers were normalized to the mean of FGF-treated control wells for each respective cell type (Fig. 2A). Consistent with our previous studies with MM14 myoblasts, proliferation in both C2C12 wild-type and C2C12 F36Vfgfr-1 cells was stimulated by bFGF treatment (100 ± 9.8 vs. 46 ± 5.8% in bFGF-treated and untreated wild-type cells, respec-

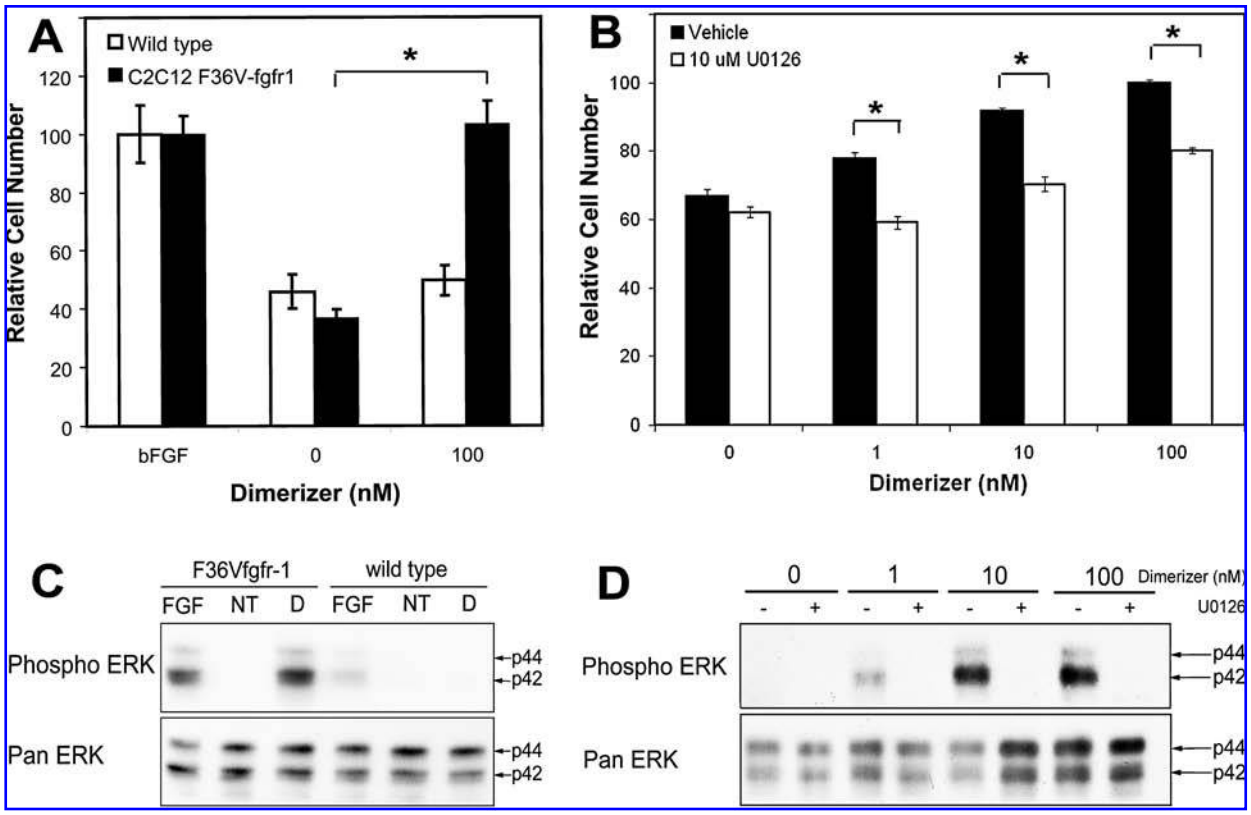

FIG. 2. C2C12 F36Vfgfr-1 cells proliferate and phosphorylate ERK in response to dimerizer treatment. (**A**) C2C12 F36Vfgfr-1 and wild-type myoblasts were treated with bFGF (6 ng/ml) or dimerizer for 48 hr. Relative cell number was normalized to the mean cell number in bFGF-treated wells of each respective cell type. C2C12 F36Vfgfr-1 cells proliferated in response to both bFGF and dimerizer treatment (*$p < 0.01$ compared with no treatment). Wild-type cells proliferated in response to bFGF but not to dimerizer. (**B**) C2C12 F36Vfgfr-1 cells were treated with 0, 1, 10, or 100 n*M* dimerizer with or without the MEK inhibitor U0126 for 48 hr. C2C12 F36Vfgfr-1 cells proliferated in response to dimerizer in a dose-dependent fashion. Dimerizer-mediated proliferation was inhibited by U0126 at all dimerizer doses (*$p < 0.01$). Data shown represent means ± standard error of three wells for each treatment in (**A**) and (**B**). (**C**) C2C12 wild-type and C2C12 F36Vfgfr-1 cells were serum starved overnight and treated for 15 min with bFGF, received no treatment (NT), or were treated with 100 n*M* dimerizer (D). Western blotting was performed to assess ERK-1/2 phosphorylation. ERK phosphorylation was induced in both C2C12 F36Vfgfr-1 cells and wild-type cells in response to bFGF. ERK was not phosphorylated in cells that received no treatment. ERK-1/2 was phosphorylated in dimerizer-treated C2C12 F36Vfgfr-1 cells but not in C2C12 wild-type cells. (**D**) C2C12 F36Vfgfr-1 cells were serum starved overnight and treated for 15 min with 0, 1, 10, or 100 n*M* dimerizer with or without the MEK inhibitor U0126. Western blotting was performed to assess ERK-1/2 phosphorylation. C2C12 F36Vfgfr-1 cells had greater ERK-1/2 phosphorylation after 10 versus 1 n*M* dimerizer treatment. Levels of ERK-1/2 phosphorylation appeared to plateau between 10 and 100 n*M* dimerizer treatment. U0126 administration inhibited ERK-1/2 phosphorylation at all dimerizer doses.

tively, and 100 ± 6.4 vs. 37 ± 3.2%, in bFGF-treated and untreated F36Vfgfr-1 cells, respectively; Fig. 2A). When F36Vfgfr-1 cells were treated with dimerizer, proliferation was stimulated comparably to bFGF treatment (103 ± 7.9% of the bFGF-stimulated value for 100 n*M* dimerizer; $p < 0.05$ for nontreated vs. dimerizer; p = NS [not significant] for bFGF vs. dimerizer). In contrast, the C2C12 wild-type cells did not proliferate in response to 100 n*M* dimerizer (50 ± 5.2% of bFGF-stimulated value). Thus, chemical dimerization of the F36Vfgfr-1 receptor induced myoblast proliferation similar to treatment with bFGF, whereas wild-type myoblasts were unresponsive to dimerizer treatment.

To test the dose dependence of dimerizer-mediated proliferation, C2C12 F36Vfgfr-1 cells were also cultured for 48 hr in the presence of 0, 1, 10, or 100 n*M* dimerizer (Fig. 2B). Dimerizer stimulated C2C12 F36Vfgfr-1 proliferation in a dose-dependent fashion (67 ± 1.9, 78 ± 1.8, 92 ± 0.9, 100 ± 0.7%, respectively).

C2C12 F36Vfgfr-1 cells activate MAP kinase signaling in vitro *with dimerizer treatment*

To determine whether dimerizer and bFGF activated similar signaling pathways, C2C12 F36Vfgfr-1 and wild-type cells were stimulated with bFGF, dimerizer, or vehicle, and Western blots of cell lysates were probed with antibodies recognizing pan ERK-1/2 (loading control) or the phosphorylated forms of ERK-1/2 (Fig. 2C). Consistent with our previous studies, both C2C12 F36Vfgfr-1 and wild-type cells had low ERK-1/2 phosphorylation in the unstimulated state, and both cell populations showed ERK-1/2 phosphorylation within 15 min of bFGF treatment. The F36Vfgfr-1 myoblasts showed greater ERK phosphorylation after bFGF treatment than did wild-type cells, similar to our previous findings in MM14 myoblasts (Whitney *et al*., 2001). Dimerizer treatment induced strong ERK-1/2 phosphorylation in C2C12 F36Vfgfr-1 cells, whereas no increase was detected in wild-type cells. Hence, treatment with the dimerizer activated the MAP kinase pathway in C2C12 cells expressing the chimeric receptor comparably to treatment with bFGF.

To test whether increasing dimerizer dosage resulted in increased levels of phosphorylated ERK-1/2, C2C12 F36Vfgfr-1 cells were treated with 1 to 100 n*M* dimerizer with or without the MEK inhibitor U0126 (Fig. 2D). C2C12 F36Vfgfr-1 cells showed ERK phosphorylation in response to 1 n*M* dimerizer treatment, which was further increased with 10 n*M* dimerizer. Levels of ERK phosphorylation appeared to plateau between 10 and 100 n*M* dimerizer treatment. Inhibition of MEK with U0126 attenuated ERK phosphorylation at all dimerizer doses. Similarly, MEK inhibition reduced proliferation of C2C12 F36Vfgfr-1 cells at all dimerizer doses (Fig. 2B). Thus, dimerization of F36Vfgfr-1 activates ERK-1/2 in an MEK-dependent manner.

Enhanced in vivo *myoblast proliferation in response to dimerizer in a subcutaneous graft model*

We established a subcutaneous grafting model to determine whether myoblast proliferation could be controlled in a simple *in vivo* model and to establish dosing regimens for dimerizer treatment. MM14 F36Vfgfr-1 cells were injected subcutaneously into the backs of nude mice receiving dimerizer at 0, 9.6, or 24 mg/kg/day, and mice were killed 6 days postengraftment. Mice were injected intraperitoneally with BrdU 1 hr before sacrifice. The number of desmin and BrdU double-positive cells was determined as a percentage of the total number of desmin-positive cells (Fig. 3). In the absence of dimerizer, 4.0 ± 0.6% of myoblasts were synthesizing DNA at the time of sacrifice. Myoblast proliferation appeared to be enhanced in animals receiving dimerizer at 9.6 mg/kg/day (7.1 ± 1.1%), but this trend did not reach statistical significance. Proliferation was significantly enhanced in animals receiving dimerizer at 24 mg/kg/day (9.7 ± 1.0%, $p < 0.05$) compared with those receiving no treatment. Proliferation of MM14 F36Vfgfr-1 myoblasts grafted subcutaneously *in vivo* was therefore enhanced in a dose-dependent manner with dimerizer treatment.

Increased intracardiac graft size in animals treated with dimerizer

We initially sought to control intracardiac graft size in infarcted mouse hearts using MM14 F36Vfgfr-1 skeletal myoblasts and dimerizer. Poor MM14 skeletal myoblast survival in the ischemic environment of infarcted mouse hearts precluded the use of this cell type in our model system (unpublished data).

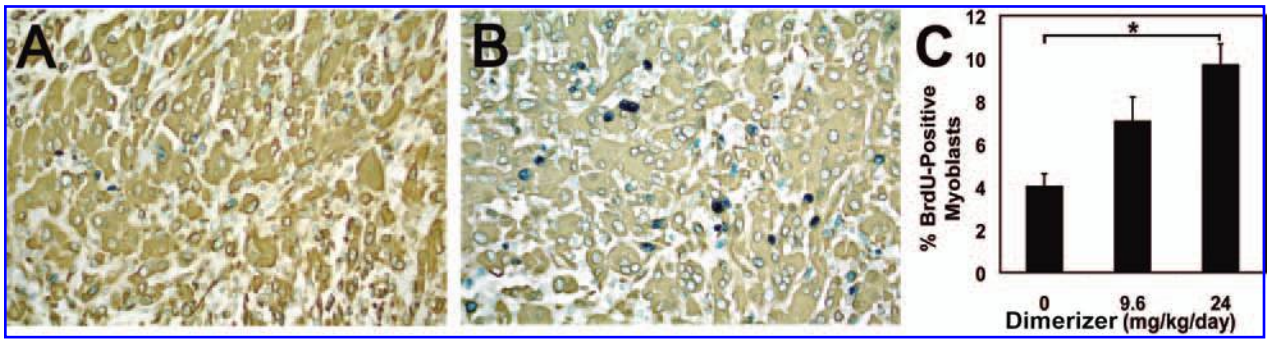

FIG. 3. MM14 F36Vfgfr-1 myoblasts proliferate in response to dimerizer in subcutaneous ectopic graft implantation model. Representative subcutaneous MM14 F36Vfgfr-1 graft sections from mice receiving no dimerizer (0 mg/kg/day) (**A**) and dimerizer at 24 mg/kg/day (**B**) are shown (desmin immunostaining, brown; BrdU nuclear immunostaining, dark blue/purple; ×40 objective). MM14 F36Vfgfr-1 myoblasts proliferated in response to dimerizer in a dose-dependent manner (**C**). Data represent means ± standard error from each of 6–11 sections from $n = 5$ (0 and 24 mg/kg/day) or $n = 3$ (9.6 mg/kg/day) subcutaneous grafts (*$p < 0.05$ for 0- vs. 24-mg/kg/day dose).

C2C12 F36Vfgfr-1 cells were therefore injected into infarcted hearts of nude mice receiving dimerizer at 0, 9.6, or 24 mg/kg/day delivered over a 7-day period via osmotic pumps. Mice were killed 6 or 24 days after cell injection and graft cells were identified by immunohistochemical staining for embryonic skeletal myosin (Fig. 4). Representative histological sections from mice killed at 6 and 24 days are shown in Fig. 4. At 6 days after cell injection, intracardiac grafts appeared to be larger in mice receiving vehicle (5.0 ± 1.1% of the left ventricle) than in those receiving dimerizer (3.2 ± 1.0%), but this trend was not significant ($p > 0.05$, $n = 5$ and 7 per group, respectively). At 24 days after cell injection, intracardiac graft size in animals receiving vehicle was 20 ± 2.7% of the left ventricle ($n = 11$). Animals receiving dimerizer at 9.6 mg/kg/day ($n = 2$) or 24 mg/kg/day ($n = 7$) had grafts that were significantly larger than those in animals receiving vehicle only (40.4 ± 6.8 and 42.9 ± 4.3%, respectively; $p < 0.01$; approximately 2-fold increase over vehicle-treated animals). Grafts were not significantly different in size ($p > 0.05$) between animals treated with dimerizer at 9.6 or 24 mg/kg/day, although small group size in the low-dose dimerizer group limits statistical power. Embryonic myosin-positive grafts were composed of well-differentiated, multinucleated myotubes with clearly identifiable sarcomeres in all animals killed 24 days after cell injection (Fig. 4G). In summary, animals treated with dimerizer hosted significantly larger intracardiac cell grafts 24 days after cell injection.

Improved graft–host apposition in animals treated with dimerizer

Collagen content and organization of C2C12 cell grafts in infarcted nude mouse hearts were assessed by sirius red and fast green staining (Fig. 5). Total collagen in grafts was similar between animals receiving vehicle only and dimerizer treatment (19.5 ± 2.7 vs. 21.9 ± 3.8 mm^2, respectively; $p > 0.05$). Percentage of collagen in the graft area, an index of graft collagen density, tended to be reduced in animals receiving dimerizer compared with vehicle only (12.6 ± 2.9 vs. 18.7 ± 2.6%, respectively; $p > 0.05$). Qualitatively, grafts in vehicle-treated animals were surrounded and infiltrated by bundles of densely packed collagen fibers, and this fibrous tissue formed a barrier between grafts and host myocardium. In contrast, dimerizer-treated animals had small, less densely packed collagen fibers within and around the grafts, and there was considerably reduced fibrosis at the graft–host interface. Hence, total infarct collagen content was similar between animals receiving vehicle and dimerizer, but this collagen tended to be more diffuse and was distributed throughout the interstitial space in the larger grafts of animals treated with dimerizer.

Reduced postinfarct ventricular dilation in animals treated with dimerizer

Postinfarct remodeling was assessed by M-mode echocardiography at the level of the midpapillary muscle (Fig. 6). Interestingly, at 2 days postinfarction all of the cell-treated groups showed a modest attenuation in left ventricular dilation compared with the sham-injected group ($p < 0.05$), although there was no effect of dimerizer treatment at this time. The left ventricular chamber dilated significantly between days 2 and 24 in infarcted, sham-engrafted mice (LVEDD, 4.2 ± 0.1 vs. 5.3 ± 0.3 mm [$p < 0.05$]; LVESD, 3.4 ± 0.1 vs. 4.9 ± 0.4 mm

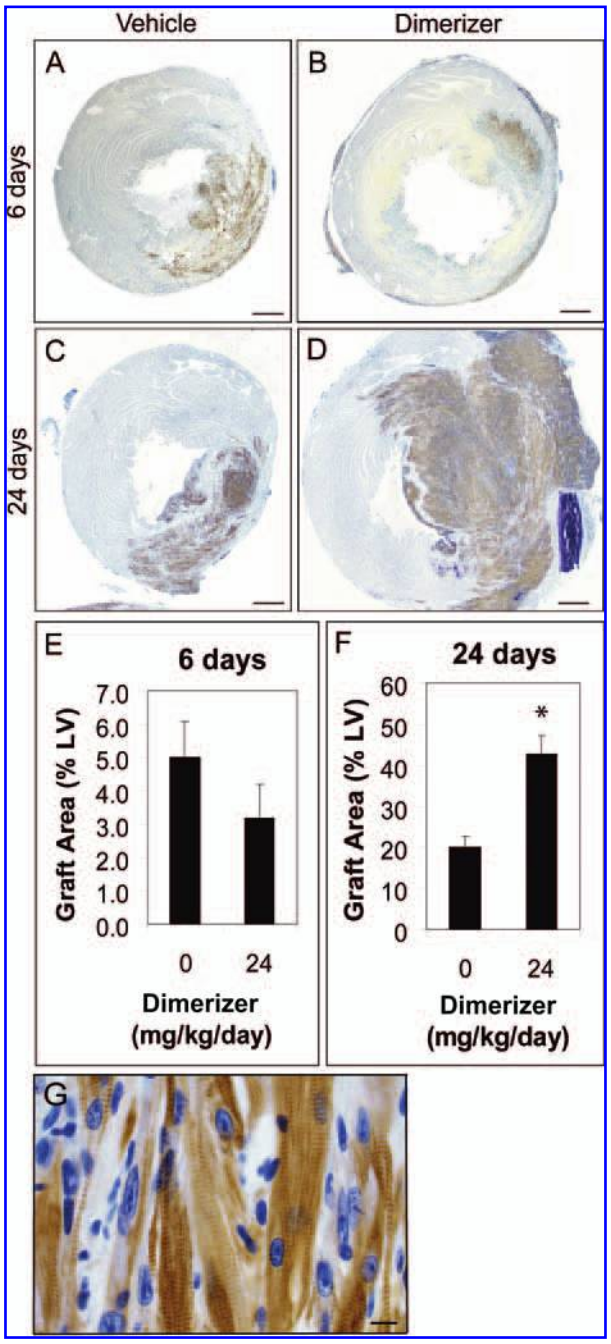

FIG. 4. Dimerizer treatment enhances long-term graft size. Transfected C2C12 F36Vfgfr-1 cells were injected into infarcted hearts of nude mice receiving dimerizer at 0, 9.6, or 24 mg/kg/day via osmotic pumps. Mice were killed 6 or 24 days after cell injection. Representative sections from hearts of animals killed on day 6 receiving vehicle (**A**) or dimerizer at 24 mg/kg/day (**B**) (embryonic skeletal myosin immunostaining, brown). Representative sections of hearts from animals killed at 24 days receiving vehicle only (**C**) or dimerizer at 24 mg/kg/day (**D**). Animals receiving dimerizer tended to have smaller cell grafts by 6 days after cell injection (**E**) and had significantly (*$p < 0.01$) larger grafts at 24 days after cell injection (**F**). Note that the graft in (**D**) is adhered to a portion of the chest wall containing a rib (dark purple object). Graft cells at 24 days were well differentiated and contained sarcomeres (**G**). Scale bars: (**A–D**) 500 μm; (**G**) 10 μm.

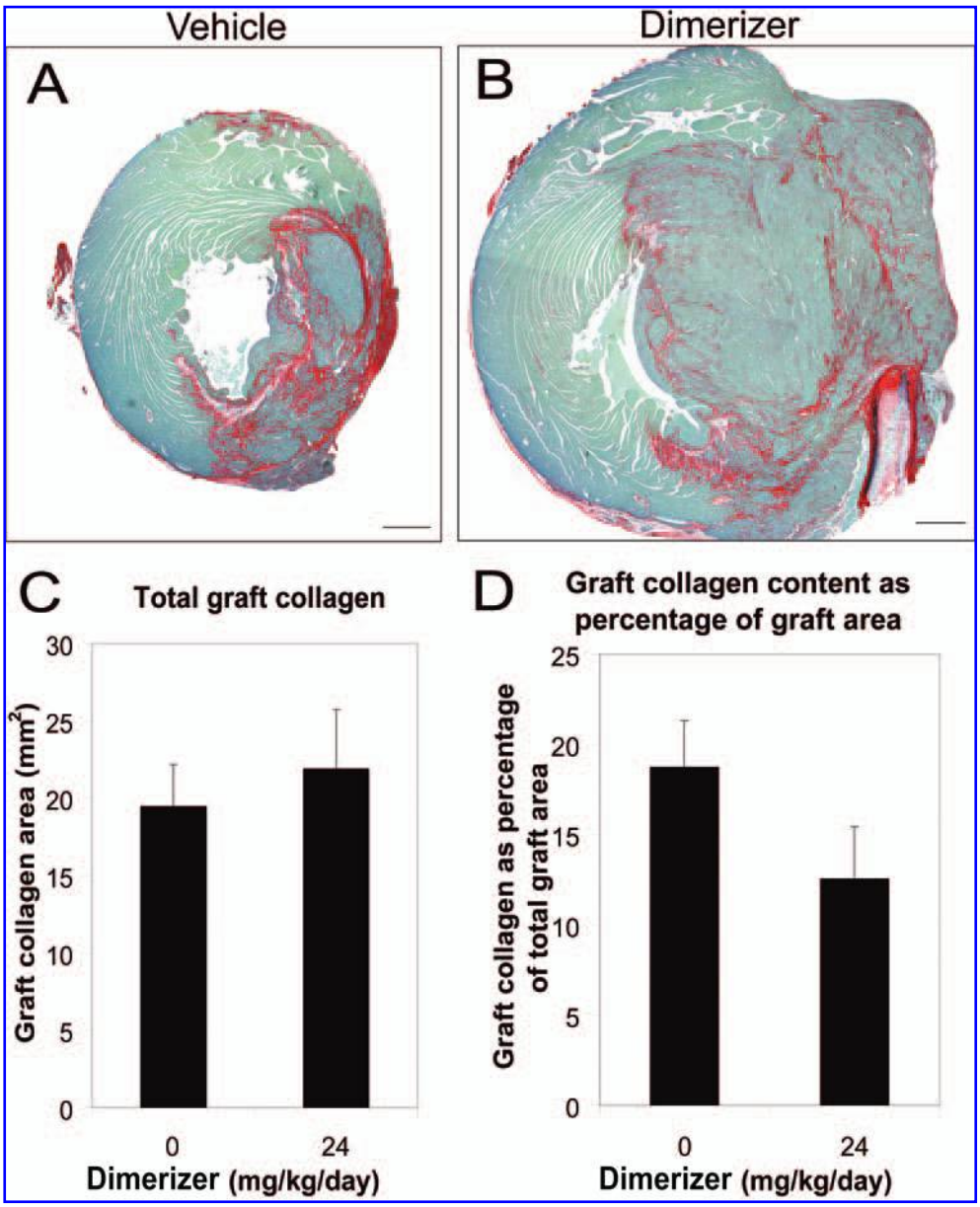

FIG. 5. Improved graft–host interface and reduced graft collagen density. Myocardial collagen content in the infarcted hearts of nude mice receiving C2C12 F36Vfgfr-1 cells and dimerizer was assessed by sirius red (collagen fibers) and fast green (other tissue elements) staining. Collagen was more densely packed in and around grafts of animals receiving vehicle only (**A**) compared with grafts of animals receiving dimerizer at 24 mg/kg/day (**B**). Graft–host apposition also appeared to be improved in animals receiving dimerizer. Total graft collagen content was similar between animals that received vehicle compared with those receiving dimerizer (**C**). Collagen content expressed as a percentage of graft area tended to be reduced in animals receiving dimerizer (**D**), but this reduction was not statistically significant ($p > 0.05$). Scale bars: 500 μm.

FIG. 6. Reduced postinfarct ventricular dilation in C2C12 F36Vfgfr-1-engrafted animals receiving dimerizer. Myocardial function was assessed by echocardiography 2 and 24 days after coronary artery ligation and intracardiac injection of C2C12 F36Vfgfr-1 cells. Left ventricular end diastolic dimension (LVEDD) and left ventricular end systolic dimension (LVESD) were measured from short axis M-mode images at the level of the midpapillary muscle in a blinded fashion. Between days 2 and 24 postinfarction, left ventricular dimensions increased significantly in mice receiving no cells and also in mice that received cells and vehicle only ($p < 0.05$). In contrast, ventricular dilation was attenuated in animals receiving cells and dimerizer at 9.6 mg/kg/day ($n = 2$). Chamber dimension decreased significantly between days 2 and 24 in mice receiving both cells and dimerizer at 24 mg/kg/day ($p < 0.01$) (**A**). Representative M-mode images from mice receiving sham injections (infarct without cell transplantation) (**B**) or C2C12 F36Vfgfr-1 cell injections and vehicle (**C**) or dimerizer at 24 mg/kg/day (**D**). (**E** and **F**) Expansion of heart rhythm strips from animals shown in (**C**) and (**D**), respectively. Note marked left ventricular dilation and anterior wall akinesis due to myocardial infarction in (**B**), the thickened noncontractile anterior wall region corresponding to a large cell graft in (**D**), and arrhythmias (irregularly timed contractions) in (**F**).

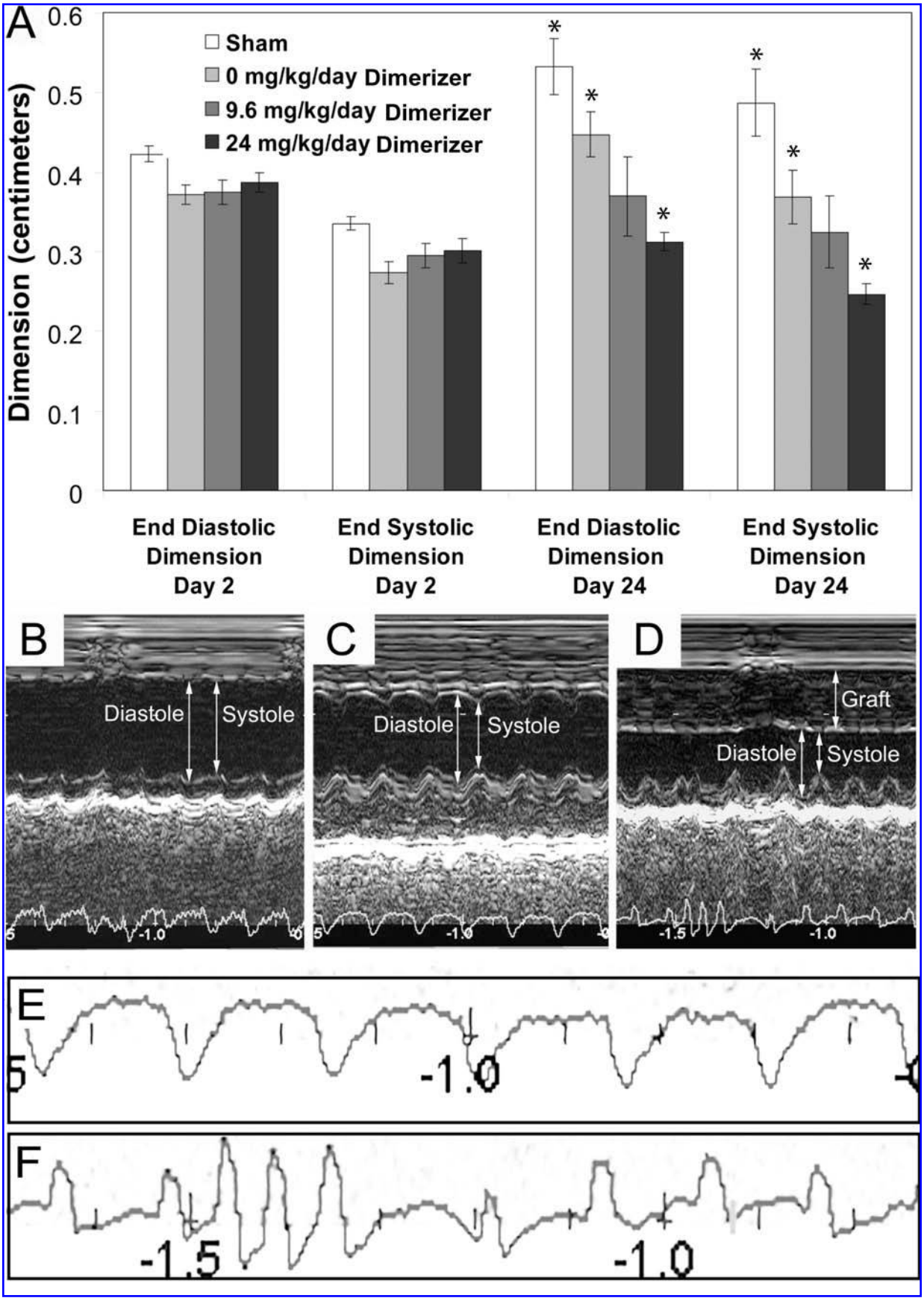
A
Dimension (centimeters)
0.6
0.5
0.4
0.3
0.2
0.1
0
Sham
0 mg/kg/day Dimerizer
9.6 mg/kg/day Dimerizer
24 mg/kg/day Dimerizer
*
End Diastolic Dimension Day 2
End Systolic Dimension Day 2
End Diastolic Dimension Day 24
End Systolic Dimension Day 24
B
Diastole
Systole
-1.0
C
Diastole
Systole
-1.0
D
Graft
Diastole
Systole
-1.5
-1.0
E
-1.0
F
-1.5
-1.0

[$p < 0.01$]). Chamber dilation, albeit attenuated, was also observed in mice that received cells and vehicle only between 2 and 24 days (LVEDD, 3.7 ± 0.1 vs. 4.5 ± 0.3 mm [$p < 0.05$]; LVESD, 2.7 ± 0.1 vs. 3.7 ± 0.3 mm [$p < 0.01$]). In contrast to sham or cell-engrafted plus vehicle mice, the left ventricles did not dilate significantly between days 2 and 24 in animals receiving C2C12 F36Vfgfr-1 cells and dimerizer at 9.6 mg/kg/day (LVEDD, 3.8 ± 0.2 vs. 3.7 ± 0.5 mm; LVESD, 3.0 ± 0.2 vs. 3.3 ± 0.5 mm). Reduction in left ventricular dilation was most impressively observed between days 2 and 24 in mice receiving both cells and dimerizer at 24 mg/kg/day (LVEDD, 3.9 ± 0.1 vs. 3.1 ± 0.1 mm [$p < 0.01$]; LVESD, 3.0 ± 0.2 vs. 2.5 ± 0.2 mm [$p < 0.01$]). The grafts in dimerizer-treated mice were readily visualized by two-dimensional analysis, and it was clear that they were noncontractile. Furthermore, in the high-dose dimerizer group, all animals except one (six of seven) had arrhythmias composed of premature ventricular contractions or runs of ventricular tachycardia. One of 11 animals that received a myoblast graft but no dimerizer had similar arrhythmias. Interestingly, this animal had the largest graft in the control group. The difference in proportion of animals exhibiting arrhythmias in vehicle versus dimerizer (24 mg/kg/day)-treated animals was statistically significant. Hence, echocardiography demonstrated that chemical dimerization of the FGF receptor in graft cells *in vivo* was associated with dose-dependent reductions in left ventricular dilation, accompanied by increased arrhythmias, after myocardial infarction.

DISCUSSION

In the present study, mouse skeletal myoblasts engineered to express the F36Vfgfr-1 chimeric receptor were treated with a synthetic molecule that induces receptor dimerization *in vitro* and *in vivo*. C2C12 F36Vfgfr-1 cells activated the MAP kinase pathway and proliferated in response to dimerizer similar to treatment with bFGF. Furthermore, C2C12 F36Vfgfr-1 graft cells withdrew from the cell cycle and differentiated *in vitro* (data not shown) and *in vivo* after dimerizer withdrawal, indicating that the signaling pathway is reversible. Dimerizer administration stimulated the proliferation of subcutaneous ectopic MM14 F36Vfgfr-1 graft cells in a dose-dependent manner. Administration of dimerizer augmented intracardiac C2C12 F36Vfgfr-1 graft size in infarcted hearts of nude mice. Echocardiography demonstrated that dose-dependent increases in myoblast graft size with dimerizer treatment were associated with corresponding dose-dependent reductions in ventricular dilation after myocardial infarction.

To our knowledge, these results represent the first demonstration of controlled graft proliferation in the setting of cell-based cardiac repair. Interestingly, at day 6 after cell injection, grafts in animals receiving vehicle tended to be larger than grafts in dimerizer-treated animals. Skeletal myoblasts undergo substantial hypertrophy after differentiation, and thus graft size does not necessarily correlate with cell number before the terminal differentiation of grafted cells. In our experiments, dimerizer was administered until 6 days after cell injection. At this time point, graft cells in vehicle-treated animals likely exited the cell cycle, differentiated, and grew larger than their more proliferative counterparts that were still exposed to dimerizer on day 6. These results agree with previous studies showing that untreated skeletal myoblasts proliferate in infarcted hearts for approximately 3 days before they withdraw from the cell cycle and form well-differentiated skeletal muscle grafts (Murry *et al*., 1996). By day 24 after cell injection, dimerizer elution would have long since terminated, and graft cells in dimerizer-treated animals would have also withdrawn from the cell cycle, fused into myotubes, and hypertrophied. After differentiation was complete in both groups, animals that received dimerizer had significantly larger intracardiac grafts compared with those receiving vehicle only.

Large intracardiac grafts in animals receiving dimerizer were clearly visible and noncontractile by echocardiography. Despite the noncontractile nature of the graft, increasing dosages of dimerizer were associated with dose-dependent reductions in ventricular dilation after myocardial infarction. This suggests that systolic force generation is not responsible for graft-induced reduction in postinfarct remodeling. Instead, it is likely that the grafts prevented infarct wall thinning and thereby normalized wall stress, which in turn prevented ventricular dilation. We noted that ventricular dimensions were significantly reduced in all animals that received cells (regardless of dimerizer treatment) at only 2 days after myocardial infarction. This suggests that paracrine factors released by graft cells or other unidentified mechanisms may also have contributed to reduced ventricular remodeling.

Echocardiography also demonstrated prevalent arrhythmias (typically ventricular tachycardia or premature ventricular contractions) in all but one animal receiving dimerizer. Dimerizer-treated animals had significantly larger skeletal myoblast grafts than their vehicle-treated counterparts, suggesting that animals with larger grafts were more susceptible to the development of arrhythmias. Interestingly, the single animal in the vehicle-treated group exhibiting arrhythmias also had the largest graft of its group. Increased arrhythmogenesis due to larger graft size would not be surprising because skeletal myoblasts form mature skeletal muscle (not cardiomyocytes) after injection into the heart (Reinecke *et al*., 2002), do not express gap junctions, and do not form electromechanical junctions with cardiomyocytes (Reinecke *et al*., 2002; Hagege *et al*., 2003; Rubart *et al*., 2004). In fact, ventricular tachycardia was observed in patients in several early clinical trials of skeletal myoblasts for cardiac repair (Menasche *et al*., 2001, 2003; Herreros *et al*., 2003; Pagani *et al*., 2003; Smits *et al*., 2003; Siminiak *et al*., 2004; Hagege *et al*., 2006). In addition, Fernandes *et al*. reported increased inducibility of ventricular arrhythmias in infarcted rat hearts injected with myoblasts compared with those receiving sham injections or autologous bone marrow mononuclear cell injections (Fernandes *et al*., 2006). On the basis of this information, we hypothesize that the significantly larger skeletal muscle grafts in dimerizer-treated animals in our study, by virtue of their being electrically insulated from the host myocardium, altered impulse propagation and promoted reentrant pathways. However, enhanced local automaticity cannot be ruled out with the current data. This model is, to our knowledge, the first animal model to demonstrate predictable spontaneous arrhythmias after cell transplantation in the heart, and as such it may prove useful in determining the pathogenesis and treatment of these arrhythmias.

Our results suggest that dimerizer-mediated graft cell proliferation controls not only graft size and heart dimensions, but

also matrix remodeling and fibrosis in postinfarct hearts. Although total graft collagen content was the same between groups, collagen was less dense and organized in grafts of animals treated with dimerizer. Importantly, graft–host apposition also appeared to be improved in animals treated with dimerizer, suggesting that cell grafts in dimerizer-treated animals could be better poised to interact with host tissue. Such apposition would be particularly beneficial for graft cells other than skeletal myoblasts that can electromechanically couple with host myocardium, such as cardiomyocytes (Rubart *et al*., 2003).

Controlling graft cell proliferation should permit a smaller number of cells to be injected initially and then expanded to a therapeutically beneficial level *in vivo*. Our system, which selectively controls the proliferation of genetically modified graft cells in infarcted hearts with a small molecule, is a step in that direction. Although promising, much work is yet to be done before this strategy could be translated to the clinic. The importance of determining the appropriate dose and duration of dimerizer administration after cell engraftment is evident, given that at the highest dosage of dimerizer bulky grafts sometimes intruded on and distorted heart borders. This is consistent with previous "overdose" studies that also used ischemia-resistant skeletal myoblasts as graft cells (Reinecke and Murry, 2000). Careful dosing studies must be performed to ensure that graft size can be optimized to attain maximal therapeutic benefit. Early online monitoring of graft size by an imaging modality (Cao *et al*., 2006) or biochemical marker could allow for optimization of dimerizer dosing and delivery based on actual graft size. This strategy may be applied to other cell types that could be more suitable for intramyocardial grafting than skeletal myoblasts, which, despite their positive effect on left ventricular remodeling, might result in arrhythmia generation. Ideal graft cell populations for cardiac repair, to which this system may be adapted, would generate new cardiomyocytes and have proliferative capacity. Our group has shown that human embryonic stem cell-derived cardiomyocytes proliferate *in vitro* (McDevitt, 2004) and after engraftment into nude rat hearts (Laflamme *et al*., 2005). Coupling of human embryonic stem cell-derived cardiomyocyte transplantation with the dimerizer-mediated *in situ* proliferation strategy developed in the present study could have a powerful impact on cardiac repair after myocardial infarction.

ACKNOWLEDGMENTS

The authors thank Veronica Muskheli, Julia Reece, and Kira Bendixen for help with animal husbandry, immunohistochemistry, and morphometry. This work was supported by NIH grants HL3174, HL64387, HL61553, and HL84642. K.R.S. was supported by an NSF graduate research fellowship and a Bioengineering Cardiovascular Training Grant (NIH EB001650). M.W.R. and M.B.N. were supported by a Cardiovascular Pathology Training Grant (NIH HL07312).

AUTHOR DISCLOSURE STATEMENT

No competing financial interests exist.

REFERENCES

BOILLY, B., VERCOUTTER-EDOUART, A.S., HONDERMARCK, H., NURCOMBE, V., and LE BOURHIS, X. (2000). FGF signals for cell proliferation and migration through different pathways. Cytokine Growth Factor Rev. **11,** 295–302.

CAO, F., LIN, S., XIE, X., RAY, P., PATEL, M., ZHANG, X., DRUKKER, M., DYLLA, S.J., CONNOLLY, A.J., CHEN, X., WEISSMAN, I.L., GAMBHIR, S.S., and WU, J.C. (2006). *In vivo* visualization of embryonic stem cell survival, proliferation, and migration after cardiac delivery. Circulation **113,** 1005–1014.

CLACKSON, T., YANG, W., ROZAMUS, L.W., HATADA, M., AMARA, J.F., ROLLINS, C.T., STEVENSON, L.F., MAGARI, S.R., WOOD, S.A., COURAGE, N.L., LU, X., CERASOLI, F., Jr., GILMAN, M., and HOLT, D.A. (1998). Redesigning an FKBP–ligand interface to generate chemical dimerizers with novel specificity. Proc. Natl. Acad. Sci. U.S.A. **95,** 10437–10442.

FERNANDES, S., AMIRAULT, J.C., LANDE, G., NGUYEN, J.M., FOREST, V., BIGNOLAIS, O., LAMIRAULT, G., HEUDES, D., ORSONNEAU, J.L., HEYMANN, M.F., CHARPENTIER, F., and LEMARCHAND, P. (2006). Autologous myoblast transplantation after myocardial infarction increases the inducibility of ventricular arrhythmias. Cardiovasc. Res. **69,** 348–358.

HAGEGE, A.A., CARRION, C., MENASCHE, P., VILQUIN, J.T., DUBOC, D., MAROLLEAU, J.P., DESNOS, M., and BRUNEVAL, P. (2003). Viability and differentiation of autologous skeletal myoblast grafts in ischaemic cardiomyopathy. Lancet **361,** 491–492.

HAGEGE, A.A., MAROLLEAU, J.P., VILQUIN, J.T., ALHERITIERE, A., PEYRARD, S., DUBOC, D., ABERGEL, E., MESSAS, E., MOUSSEAUX, E., SCHWARTZ, K., DESNOS, M., and MENASCHE, P. (2006). Skeletal myoblast transplantation in ischemic heart failure: Long-term follow-up of the first phase I cohort of patients. Circulation **114,** I108–I113.

HERREROS, J., PROSPER, F., PEREZ, A., GAVIRA, J.J., GARCIA-VELLOSO, M.J., BARBA, J., SANCHEZ, P.L., CANIZO, C., RABAGO, G., MARTI-CLIMENT, J.M., HERNANDEZ, M., LOPEZ-HOLGADO, N., GONZALEZ-SANTOS, J.M., MARTIN-LUENGO, C., and ALEGRIA, E. (2003). Autologous intramyocardial injection of cultured skeletal muscle-derived stem cells in patients with non-acute myocardial infarction. Eur. Heart J. **24,** 2012–2020.

KOH, G.Y., KLUG, M.G., SOONPAA, M.H., and FIELD, L.J. (1993). Differentiation and long-term survival of C2C12 myoblast grafts in heart. J. Clin. Invest. **92,** 1548–1554.

LAFLAMME, M.A., GOLD, J., XU, C., HASSANIPOUR, M., ROSLER, E., POLICE, S., MUSKHELI, V., and MURRY, C.E. (2005). Formation of human myocardium in the rat heart from human embryonic stem cells. Am. J. Pathol. **167,** 663–671.

LI, R.K., JIA, Z.Q., WEISEL, R.D., MICKLE, D.A., ZHANG, J., MOHABEER, M.K., RAO, V., and IVANOV, J. (1996). Cardiomyocyte transplantation improves heart function. Ann. Thorac. Surg. **62,** 654–660; discussion 660–651.

MANGI, A.A., NOISEUX, N., KONG, D., HE, H., REZVANI, M., INGWALL, J.S., and DZAU, V.J. (2003). Mesenchymal stem cells modified with Akt prevent remodeling and restore performance of infarcted hearts. Nat. Med. **9,** 1195–1201.

McDEVITT, T.C., LAFLAMME, M.A., and MURRY, C.E. (2005). Proliferation of cardiomyocytes derived from human embryonic stem cells is mediated via the IGF/PI 3-kinase/Akt signaling pathway. J. Mol. Cell. Cardiol. **39,** 865–873.

MENASCHE, P., HAGEGE, A.A., SCORSIN, M., POUZET, B., DESNOS, M., DUBOC, D., SCHWARTZ, K., VILQUIN, J.T., and MAROLLEAU, J.P. (2001). Myoblast transplantation for heart failure. Lancet **357,** 279–280.

MENASCHE, P., HAGEGE, A.A., VILQUIN, J.T., DESNOS, M., ABERGEL, E., POUZET, B., BEL, A., SARATEANU, S.,

SCORSIN, M., SCHWARTZ, K., BRUNEVAL, P., BENBUNAN, M., MAROLLEAU, J.P., and DUBOC, D. (2003). Autologous skeletal myoblast transplantation for severe postinfarction left ventricular dysfunction. J. Am. Coll. Cardiol. **41,** 1078–1083.

MILASINCIC, D.J., CALERA, M.R., FARMER, S.R., and PILCH, P.F. (1996). Stimulation of C2C12 myoblast growth by basic fibroblast growth factor and insulin-like growth factor 1 can occur via mitogen-activated protein kinase-dependent and -independent pathways. Mol. Cell. Biol. **16,** 5964–5973.

MURRY, C.E., WISEMAN, R.W., SCHWARTZ, S.M., and HAUSCHKA, S.D. (1996). Skeletal myoblast transplantation for repair of myocardial necrosis. J. Clin. Invest. **98,** 2512–2523.

MURRY, C.E., FIELD, L.J., and MENASCHE, P. (2005). Cell-based cardiac repair: Reflections at the 10-year point. Circulation **112,** 3174–3183.

PAGANI, F.D., DERSIMONIAN, H., ZAWADZKA, A., WETZEL, K., EDGE, A.S., JACOBY, D.B., DINSMORE, J.H., WRIGHT, S., ARETZ, T.H., EISEN, H.J., and AARONSON, K.D. (2003). Autologous skeletal myoblasts transplanted to ischemia-damaged myocardium in humans: Histological analysis of cell survival and differentiation. J. Am. Coll. Cardiol. **41,** 879–888.

POUZET, B., VILQUIN, J.T., HAGEGE, A.A., SCORSIN, M., MESSAS, E., FISZMAN, M., SCHWARTZ, K., and MENASCHE, P. (2001). Factors affecting functional outcome after autologous skeletal myoblast transplantation. Ann. Thorac. Surg. **71,** 844–850; discussion 850–841.

REINECKE, H., and MURRY, C.E. (2000). Transmural replacement of myocardium after skeletal myoblast grafting into the heart: Too much of a good thing? Cardiovasc. Pathol. **9,** 337–344.

REINECKE, H., POPPA, V., and MURRY, C.E. (2002). Skeletal muscle stem cells do not transdifferentiate into cardiomyocytes after cardiac grafting. J. Mol. Cell. Cardiol. **34,** 241–249.

RUBART, M., PASUMARTHI, K.B., NAKAJIMA, H., SOONPAA, M.H., NAKAJIMA, H.O., and FIELD, L.J. (2003). Physiological coupling of donor and host cardiomyocytes after cellular transplantation. Circ. Res. **92,** 1217–1224.

RUBART, M., SOONPAA, M.H., NAKAJIMA, H., and FIELD, L.J. (2004). Spontaneous and evoked intracellular calcium transients in donor-derived myocytes following intracardiac myoblast transplantation. J. Clin. Invest. **114,** 775–783.

SIMINIAK, T., KALAWSKI, R., FISZER, D., JERZYKOWSKA, O., RZEZNICZAK, J., ROZWADOWSKA, N., and KURPISZ, M. (2004). Autologous skeletal myoblast transplantation for the treatment of postinfarction myocardial injury: Phase I clinical study with 12 months of follow-up. Am. Heart J. **148,** 531–537.

SMITS, P.C., VAN GEUNS, R.J., POLDERMANS, D., BOUNTIOUKOS, M., ONDERWATER, E.E., LEE, C.H., MAAT, A.P., and SERRUYS, P.W. (2003). Catheter-based intramyocardial injection of autologous skeletal myoblasts as a primary treatment of ischemic heart failure: A clinical experience with six-month follow-up. J. Am. Coll. Cardiol. **42,** 2063–2069.

SUZUKI, K., SMOLENSKI, R.T., JAYAKUMAR, J., MURTUZA, B., BRAND, N.J., and YACOUB, M.H. (2000). Heat shock treatment enhances graft cell survival in skeletal myoblast transplantation to the heart. Circulation **102,** III216–III221.

TAMBARA, K., SAKAKIBARA, Y., SAKAGUCHI, G., LU, F., PREMARATNE, G.U., LIN, X., NISHIMURA, K., and KOMEDA, M. (2003). Transplanted skeletal myoblasts can fully replace the infarcted myocardium when they survive in the host in large numbers. Circulation **108**(Suppl. 1)**,** II259–II263.

TEMPLETON, T.J., and HAUSCHKA, S.D. (1992). FGF-mediated aspects of skeletal muscle growth and differentiation are controlled by a high affinity receptor, FGFR1. Dev. Biol. **154,** 169–181.

VIRAG, J.I., and MURRY, C.E. (2003). Myofibroblast and endothelial cell proliferation during murine myocardial infarct repair. Am. J. Pathol. **163,** 2433–2440.

WHITNEY, M.L., OTTO, K.G., BLAU, C.A., REINECKE, H., and MURRY, C.E. (2001). Control of myoblast proliferation with a synthetic ligand. J. Biol. Chem. **276,** 41191–41196.

YAU, T.M., LI, G., WEISEL, R.D., REHEMAN, A., JIA, Z.Q., MICKLE, D.A., and LI, R.K. (2004). Vascular endothelial growth factor transgene expression in cell-transplanted hearts. J. Thorac. Cardiovasc. Surg. **127,** 1180–1187.

ZHANG, M., METHOT, D., POPPA, V., FUJIO, Y., WALSH, K., and MURRY, C.E. (2001). Cardiomyocyte grafting for cardiac repair: Graft cell death and anti-death strategies. J. Mol. Cell. Cardiol. **33,** 907–921.

Address reprint requests to:
Dr. Charles E. Murry
Center for Cardiovascular Biology
University of Washington
815 Mercer Street,
Seattle, WA 98109

E-mail: murry@u.washington.edu

Received for publication October 26, 2006; accepted after revision March 26, 2007.

Published online: May 2, 2007.

This article has been cited by:

1. Donglu Shi, Rigwed Tatu, Qing Liu, Hossein Hosseinkhani. 2014. Stem Cell-Based Tissue Engineering for Regenerative Medicine. *Nano LIFE* **04**, 1430001. [CrossRef]
2. Jennifer D Bernet, Jason D Doles, John K Hall, Kathleen Kelly Tanaka, Thomas A Carter, Bradley B Olwin. 2014. p38 MAPK signaling underlies a cell-autonomous loss of stem cell self-renewal in skeletal muscle of aged mice. *Nature Medicine* . [CrossRef]
3. Hans Reinecke, Thomas E. Robey, John L. Mignone, Veronica Muskheli, Paul Bornstein, Charles E. Murry. 2013. Lack of thrombospondin-2 reduces fibrosis and increases vascularity around cardiac cell grafts. *Cardiovascular Pathology* **22**:1, 91-95. [CrossRef]
4. Anna V. Naumova, Vasily L. Yarnykh, Niranjan Balu, Hans Reinecke, Charles E. Murry, Chun Yuan. 2012. Quantification of MRI signal of transgenic grafts overexpressing ferritin in murine myocardial infarcts. *NMR in Biomedicine* **25**:10, 1187-1195. [CrossRef]
5. N. Kacherovsky, M. A. Harkey, C. A. Blau, C. M. Giachelli, S. H. Pun. 2012. Combination of Sleeping Beauty transposition and chemically induced dimerization selection for robust production of engineered cells. *Nucleic Acids Research* **40**:11, e85-e85. [CrossRef]
6. Kelly R. Stevens, Lil Pabon, Veronica Muskheli, Charles E. Murry. 2009. Scaffold-Free Human Cardiac Tissue Patch Created from Embryonic Stem Cells. *Tissue Engineering Part A* **15**:6, 1211-1222. [Abstract] [Full Text HTML] [Full Text PDF] [Full Text PDF with Links] [Supplemental Material]
7. L MAXIMILIANBUJA, D VELA. 2008. Cardiomyocyte death and renewal in the normal and diseased heart. *Cardiovascular Pathology* **17**:6, 349-374. [CrossRef]
8. Thomas E. Robey, Mark K. Saiget, Hans Reinecke, Charles E. Murry. 2008. Systems approaches to preventing transplanted cell death in cardiac repair. *Journal of Molecular and Cellular Cardiology* **45**:4, 567-581. [CrossRef]
9. Jerome Roncalli, Jörn Tongers, Marie-Ange Renault, Douglas W Losordo. 2008. Biological approaches to ischemic tissue repair: gene- and cell-based strategies. *Expert Review of Cardiovascular Therapy* **6**:5, 653-668. [CrossRef]
10. Charles E. Murry, Gordon Keller. 2008. Differentiation of Embryonic Stem Cells to Clinically Relevant Populations: Lessons from Embryonic Development. *Cell* **132**:4, 661-680. [CrossRef]
11. Marilyn B Nourse, Marsha W Rolle, Lil M Pabon, Charles E Murry. 2007. Selective control of endothelial cell proliferation with a synthetic dimerizer of FGF receptor-1. *Laboratory Investigation* **87**:8, 828-835. [CrossRef]